Heterolytic Bond Dissociation in Water: Why Is It So Easy for C_4H_9Cl But Not for C_3H_9SiCl?

Peifeng Su,[†] Lingchun Song,[†] Wei Wu,*[,†] Sason Shaik,*[,‡] and Philippe C. Hiberty*[,§]

Department of Chemistry, College of Chemistry and Chemical Engineering, and State Key Laboratory for Physical Chemistry of Solid Surfaces, Xiamen University, Xiamen, Fujian 361005, China, Department of Organic Chemistry and the Lise Meitner-Minerva Center for Computational Quantum Chemistry, The Hebrew University, Jerusalem 91904, Israel, and Laboratoire de Chimie Physique, Bât 490, Université de Paris-Sud, CNRS UMR 8000, 91405 Orsay, France

Received: January 14, 2008

The recently developed (Song, L.; Wu, W.; Zhang, Q.; Shaik, S. *J. Phys. Chem. A* **2004**, *108*, 6017−6024) valence bond method coupled to a polarized continuum model (VBPCM) is used to address the long standing conundrum of the heterolytic dissociation of the C−Cl and Si−Cl bonds, respectively, in tertiary-butyl chloride and trimethylsilyl chloride in condensed phases. The method is used here to compare the bond dissociation in the gas phase and in aqueous solution. In addition to the ground state reaction profile, VB theory also provides the energies of the purely covalent and purely ionic VB structures as a function of the reaction coordinate. Accordingly, the C−Cl and Si−Cl bonds are shown to be of different natures. In the gas phase, the resonance energy arising from covalent-ionic mixing at equilibrium geometry amounts to 42 kcal/mol for tertiary-butyl chloride, whereas the same quantity for trimethylsilyl chloride is significantly higher at 62 kcal/mol. With such a high value, the root cause of the Si−Cl bonding is the covalent-ionic resonance energy, and this bond belongs to the category of charge-shift bonds (Shaik, S.; Danovich, D.; Silvi, B.; Lauvergnat, D.; Hiberty, P. C. *Chem.— Eur. J.* **2005**, *11*, 6358). This difference between the C−Cl and Si−Cl bonds carries over to the solvated phase and impacts the heterolytic cleavages of the two bonds. For both molecules, solvation lowers the ionic curve below the covalent one, and hence the bond dissociation in the solvent generates the two ions, Me_3E^+ Cl^- (E = C, Si). In both cases, the root cause of the barrier is the loss of the covalent-ionic resonance energy. In the heterolysis reaction of Si−Cl, the covalent-ionic resonance energy remains large and fully contributes to the dissociation energy, thereby leading to a high barrier for heterolytic cleavage, and thus prohibiting the generation of ions. By contrast, the covalent-ionic resonance energy is smaller for the C−Cl bond and only partially contributes to the barrier for heterolysis, which is consequently small, leading readily to ions that are commonly observed in the classical S_N1 mechanism. Thus, the reluctance of R_3Si-X molecules to undergo heterolysis in condensed phases and more generally the rarity of free silicenium ions under these conditions are experimental manifestations of the charge-shift character of the Si−Cl bond.

Introduction

The heterolytic cleavage of tertiary alkyl halides to generate an alkyl cation and a halide anion in the now classical S_N1 mechanism is one of the most fundamental processes in organic chemistry. The general S_N1 mechanism for this solvolytic process follows the scheme proposed by Winstein,[1,2] as outlined in eq 1:

$$R-X \leftrightarrows R^+X^- \text{ (CIP)} \leftrightarrows R^+...X^- \text{ (SSIP)} \leftrightarrows \text{free ions, products} \quad (1)$$

Thus, in a first step, which is rate determining, the carbon-halide is heterolytically cleaved and generates a contact ion pair (CIP). Subsequently the ions are further separated, albeit not totally, to form a solvent separated ion pair (SSIP). Finally, a third step leads to free ions and/or to solvolytic products of the S_N1 reaction.

The free energy barrier for the rate-determining step of the tertiary-butyl chloride (t-BuCl) solvolysis was determined experimentally and found to be 19.5 kcal/mol in water at ambient temperature.[1] On the other hand, the depth of the potential well in which the CIP resides is still not accurately known. A thermodynamic analysis performed by Abraham[3] based on experimental data places the CIP free energy 14.5 kcal/mol above the reactant but with an uncertainty of ± 5 kcal/mol, meaning that the collapse of the CIP back to t-BuCl should encounter a barrier ranging from 0 to 10 kcal/mol, which is similar to other values obtained by NMR for ion pairs involving trityl and cycloheptatrienyl cations.[4]

Given that the propensity of R_3C-X compounds to undergo heterolysis in solution is associated with the partial ionic character of the C−X bond and the stabilities of the R_3C^+ and X^- ions, one might have thought that heterolysis should be even easier when carbon is replaced by silicon, which forms more

* To whom correspondence should be addressed. (W.W.) E-mail: weiwu@xmu.edu.cn. Fax: 86-592-2186207. Tel: 86-592-2182825. (S.S.) E-mail: sason@yfaat.ch.huji.ac.il. Fax: +(972)-2-6584680. Tel: +(972)-2-6585909. (P.C.H.) E-mail: philippe.hiberty@lcp.u-psud.fr. Fax: 33 (0)1 69 15 61 88. Tel: 33 (0)1 69 15 61 75.

[†] Xiamen University.

[‡] The Hebrew University.

[§] Université de Paris-Sud.

10.1021/jp8004647 CCC: $40.75
Published on Web 03/11/2008

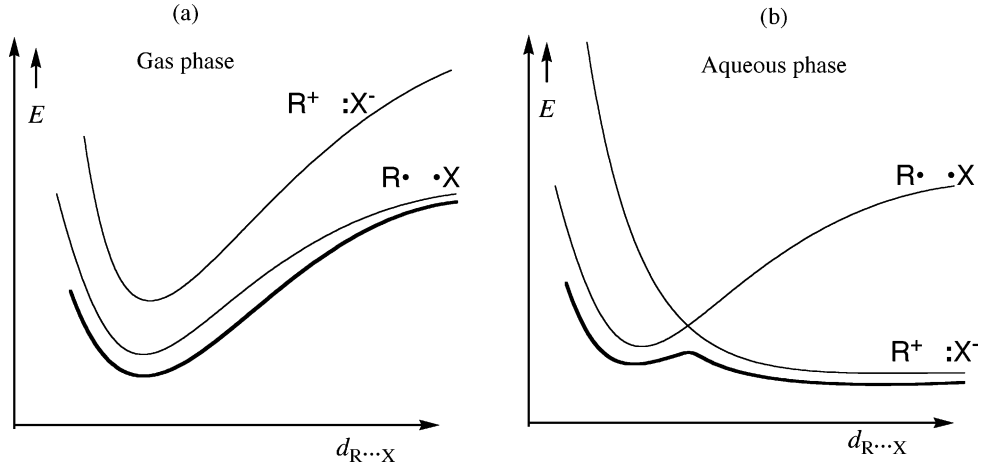

Figure 1. Schematic dissociation process according to the classical view. (a) Gas phase; (b) aqueous phase.

polar bonds than carbon. This however, is not the case; by and large R_3Si-X bonds do not undergo heterolysis in solution (but prefer to react via associative mechanisms with pentacoordinate intermediates).[5−10] In fact, the $R_3Si^+X^-$ species are so rare in condensed phases that even a compound like Ph_3SiClO_4 that might have appeared as an excellent candidate to generate a Si^+O^- bond was found to be a covalent solid exhibiting a short Si−O bond.[11] By contrast, the carbon analog is definitely ionic, $Ph_3C^+ClO_4^-$, having an Na^+Cl^- lattice type[12] Generally speaking, these are the C−X bond that exhibit ionic chemistry in condensed phases, whereas ionic Si−X chemistry is extremely rare with a handful of exceptions.[13−16] The present paper focuses on the root cause of this disparate behaviors of the two bonds.

Valence bond (VB) theory is an appropriate conceptual framework for looking at bond heterolysis problems in terms of the behaviors of the covalent and ionic components of the bond in either the gas phase or in solution, along the bond cleavage coordinate.[17−21] As shown schematically in Figure 1, the ground state adiabatic surface (the reaction surface) evolves through the mixing of the purely covalent state $R^{\bullet}-{}^{\bullet}X$ and the purely ionic one, R^+X^- (sometimes referred to as diabatic states). The mixing of the two VB structures results in stabilization of the ground state by resonance energy at the equilibrium bonding distance, and this covalent-ionic resonance energy gradually diminishes as the bond is stretched. As a consequence, the ground state merges with the lowest diabatic energy curve at long distances, but departs from it at short distances. As further shown in Figure 1a, in the gas phase the covalent structure is the lowest, and the bond dissociation results in the formation of the two radicals, $R^{\bullet}$ and $X^{\bullet}$. As shown in Figure 1b, in a solvent the ionic curve is greatly stabilized by solvation and hence facilitates a heterolytic bond breaking. The gas phase and solvated dissociation curves that are qualitatively represented in Figure 1 follow the often used assumption of relatively weak resonance energy, such that the ground state remains close to the lowest diabatic curve even at bonding distance. In accord, the classical VB approach[17] views the origin of the barrier as a result of the increased solvation of the ionic form (and not the covalent one) as the two fragments are pulled apart. As a result, the ionic curve crosses the covalent curve, and the two curves mix rather weakly and generate on the ground state a barrier that reflects the height of the crossing point. However, the assumption of weak resonance energy is not accurate and for many bonds the covalent-ionic resonance energy is very large and in some cases the dominant feature of bonding.[22] Thus, the height of the crossing point may not be at all important in gauging the barrier height. As shall be seen, the relative magnitude of the covalent-ionic resonance energy near the minimum of the ground state is precisely the reason for the different behaviors of alkyl halides and silyl halides in solution and generally in condensed phases.

A tentative explanation of the dichotomous behavior of C−X versus Si−X bonds in solution was already proposed by some of us based on VB calculations of the two bonds in the gas phase.[22] Thus, it was shown that while the C−Cl bond in H_3C-Cl is a standard polar covalent bond with a moderate covalent-ionic resonance energy, the Si−Cl bond in H_3Si-Cl exhibits a very large covalent-ionic resonance energy, which constitutes the major component of Si−Cl bonding. Bonds of this type where the covalent-ionic resonance energy dominates the bonding were referred to as belonging to the category of "charge-shift bonds".[22c] It was further postulated that due to these features, the C−Cl and Si−Cl bonds will exhibit different heterolytic behavior in solution. Thus, t-BuCl was postulated to behave as described in Figure 1b, where the ionic curve ($R_3C^+X^-$), which crosses below the covalent one ($R_3C^{\bullet}-{}^{\bullet}X$) dominates the ground state energy profile and displays a relatively small barrier to dissociation. On the other hand, in a charge-shift bond such as in Me_3Si-Cl it was postulated that the resonance energy would remain large even in the solvent, leading to significant dissociation energy even if the ionic curve is the lowest one. It was thus argued[22a,b] that the reluctance of Si−X bonds to undergo heterolysis in condensed phases is a mark of the large covalent-ionic resonance energy of charge-shift bonding.

Should these predictions turn out to be correct, there would then exist a general mechanism for understanding the disparate behavior of these bonds, and at the same time this behavior can serve as an indirect probe of the charge-shift bonding. However, a test of these predictions requires calculations of realistic systems that may undergo heterolytic cleavage in solution, namely $(CH_3)_3C-Cl$ and $(CH_3)_3Si-Cl$. Is the Si−Cl bond in the latter compound still a charge-shift bond? And does this nature indeed persist in aqueous solutions? Answering these questions is the aim of this paper, which carries out a comparative VB study of the solvolytic behavior of $(CH_3)_3C-Cl$ vis-à-vis $(CH_3)_3Si-Cl$ in aqueous solution.

An Outline of the Strategy of the Study

The solvolysis of tertiary butyl halides has been studied before using a variety of MO-, VB-, and DFT-based models where the solvent was represented in a variety of ways, starting from a small number of solvent molecules, through continuum models

SCHEME 1: VB Structures for the X−Cl (X = C, Si) Bonds

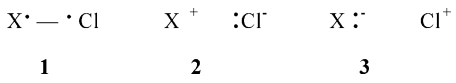

1 **2** **3**

and all the way up to a full free energy perturbation and Monte Carlo simulations.[20,23−34] To the best of our knowledge, no such comparative study of the silicon analog has been carried out, and theoretical studies of trialkyl silylium cations in solution are scarce.[35,36]

Our strategy in this paper is to use an ab initio method of valence bond type that is coupled to a continuum model (VBPCM).[23] As we already mentioned, the attractive feature of VB theory[37] is its ability to compute, in addition to the adiabatic ground state, the energy profiles of the diabatic covalent and ionic curves from which this ground state surface is constructed. In this manner, the effect of solvation of the covalent and ionic components of the bond can be readily visualized, and the covalent-ionic resonance energy as well as its contribution to the barrier can be quantified. Indeed, previous VBPCM studies in the field of ionic reactions[38−40] have demonstrated the lucid insight that one may gain into the mechanisms of chemical reactions in solution. Thus, the VB method for the gas phase and the VBPCM method for the aqueous phase will be used in the present work to investigate the effects of solvation on the diabatic and adiabatic dissociation energy curves of tert-butyl chloride and trimethylsilyl chloride (eqs 2 and 3)

$$(CH_3)_3C{-}Cl \rightarrow (CH_3)_3C^{\bullet} + Cl^{\bullet}\ (gas)\ or\ (CH_3)_3C^{+} + Cl^{-}\ (water) \quad (2)$$

$$(CH_3)_3Si{-}Cl \rightarrow (CH_3)_3Si^{\bullet} + Cl^{\bullet}\ (gas)\ or\ (CH_3)_3Si^{+} + Cl^{-}\ (water) \quad (3)$$

Theory and Methodology

The VB procedures and the VBPCM solvation model are described in detail in the Supporting Information and in previous papers.[23,38−42] Therefore, only a brief summary is outlined below.

VB Procedures. In VB theory, the state wave function, Ψ, is expressed as a linear combination of VB structures, Φ_K, in eq 4 as

$$\Psi = \sum_K C_K \Phi_K \quad (4)$$

where the Φ_K are VB structures that correspond to all the modes of distributing the "active electrons" that participate in the interchanging bonds, and the C_K are the corresponding structural coefficients. In the present work, the three VB structures that are needed to describe a dissociation process, one covalent and two ionic, are shown in Scheme 1. However, as the inverse-ionic structure $(CH_3)_3E^{-}Cl^{+}$ (E = C, Si) is highly unfavorable, only the dissociation curves of structures **1** and **2** are plotted explicitly in the subsequent figures and are called henceforth Φ_{cov}(**1**) and Φ_{ion}(**2**), respectively.

Two computational methods, VBSCF and BOVB, have been used for the ab initio VB calculations. In the VBSCF[41] procedure, both the VB orbitals and structural coefficients are optimized simultaneously to minimize the total energy. As such, the VBSCF method takes care of the static electron correlation; however, it lacks dynamic correlation that is absolutely essential for obtaining quantitative accuracy. The BOVB method[42] improves the VBSCF method by introducing dynamic correlation. In the BOVB method, the orbitals are allowed to be different for different VB structures. In this manner, the orbitals respond to the instantaneous fields of the individual VB structures rather than to an average field of all the structures. As such, the BOVB method accounts for the dynamic correlation, which is inherent in the bond making−breaking process, while leaving the wave function as compact as in VBSCF. Both methods can be used at two levels of sophistication, labeled as L- and D (L-VBSCF, L-BOVB and so on). At the L- level ("L" standing for "localized") all orbitals are strictly localized on their respective fragment, Cl or $(CH_3)_3E$ (E = C, Si). At the D-BOVB level ("delocalized"), the "spectator orbitals" (those not involved in the E−Cl bond) of π-symmetry are allowed to delocalize, resulting in more reliable bond dissociation energies. Both L- and D-levels have been used in the present work in the framework of the VBSCF and BOVB methods. A still better level called "SD" exists, but has been left aside in the present study for the sake of simplicity.

The weights of the VB structures are determined by use of the Coulson−Chirgwin formula,[43] eq 5, which is the equivalent of a Mulliken population analysis in VB theory

$$W_K = C_K^2 + \sum_{L \neq K} C_K C_L \langle \Phi_K | \Phi_L \rangle \quad (5)$$

The VBPCM Method.[23] In the PCM method, the solute molecule is studied quantum mechanically while the solute−solvent interaction is represented by an interaction potential. The VBPCM method[23] expands the state wave function Ψ in terms of the usual VB structures as in eq 4. These VB structures are optimized and allowed to interact with one another in the presence of a polarizing field of the solvent. In a similar fashion to a MO-based PCM method, the interaction between the solute and the solvent depends on the electron density of the solute and is expressed in the form of one-electron integrals. Adding these integrals to the original electronic integrals, a standard VB procedure then follows and optimizes the VB orbitals. The type of calculation will be designated henceforth by the level of calculations, for example, as VBPCM//VBSCF or VBPCM//BOVB. While the solvation process occurs in a space including an extra degree of freedom corresponding to a collective solvent coordinate,[20c] the equilibrium solvation is calculated for each value of the C(Si)−Cl bond (equilibrium solvation path approximation).

Computational Details. The equilibrium geometry and the geometries on potential surface curve are optimized at the MP2 level for the gas phase and at the Hartree−Fock level with the IEFPCM solvation model[44] for the water phase. The 6-31G(d) basis set of double-ζ + polarization type is used for the atoms that are involved in the bonds being broken, namely C, Si, and Cl, while the 6-31G basis set is used for the carbon and hydrogen atoms of the methyl groups. The original C_{3v} symmetry is kept throughout the dissociation process. All the geometry optimizations are performed with the Gaussian 98 program.[45] In the present work, the PCM part of the VB calculation was performed with the GAMESS package[46] (Version: 20 JUNE 2002 (R2)), and the VB part was done with Xiamen VB (XMVB) package.[47] An interface was written to transfer to input/output files between the two codes.

The VBPCM method is used in conjunction with the UAHF model[44] implemented in the Gaussian 98 package. The molecular cavities are defined by using standard UAHF radii for the methyl groups. For the silicon and chlorine atoms and for the carbon atom involved in the E−Cl bond, a reasonable choice

TABLE 1: The Dissociation Energy[a] and Dissociation Free Energy[a] of $(CH_3)_3C-Cl$ in Gas Phase and Aqueous Phase

		gas phase		aqueous phase		
entry	method/author	*E*	*G*[b]	*E*	*G*[c,d]	ref
1	L-VBSCF	58.7	44.9			this work
2	D-VBSCF	65.4	51.6	25.1	11.5	this work
3	L-BOVB	68.2	54.4			this work
4	D-BOVB	75.6	61.8	35.2	21.6	this work
5	HF	57.6	43.8	15.6	2.0	this work
6	CCSD(T)	81.1	67.3	37.1	23.5	this work
7	Ford				20.5	(25)
8	Kikuchi				20	(26)
9	Merz				17.8,[e,f] 23.4[e,g]	(28)
10	Okuno				28.4[e,h]	(33)
11	Watanabe				28.5[e]	(29)
12	Keirstead				20[e]	(30)
13	Rossky				23[e]	(31)
14	Winter				20.5[e]	(32)
15	Jorgensen				19.5[e]	(27)
16	expt	86.2[i]			19.5[e,j]	(NIST, 1)

[a] Energies in kcal/mol. [b] Thermal correction in VB and MO results comes from MP2/6-31G(d). [c] Thermal correction in VB and MO results comes from HF/IEFPCM/6-31G(d). [d] Nonelectrostatic solvation free energy terms come from HF/IEFPCM. [e] Free energy of the transition state between the t-BuCl minimum and the CIP intermediate. [f] With Born correction. [g] With charge correction. [h] Including ZPE correction, but not thermal correction. [i] NIST Computational Chemistry Comparison and Benchmark Database, NIST Standard reference Database N° 101, Release 10 (Eds. R. D. Johnson, III), May 2004, srdata.nist.gov/cccbdb. Calculated as DH_f^0 (experimental) + DZPE (calculated at the CCD/6-31G(d) level). [j] Ref 1.

for the atomic radii in the ground state should take into account the fact that the atomic net charges in the ground state vary throughout the reaction coordinate. This is done by defining the atomic radii as weighted functions of the atomic charges. Furthermore, as implied by the assumption that the solvent conformation is the same for the ground state and diabatic states, the same radii are used for the ground and for the diabatic curves. All radii are tabulated in Supporting Information.

In the VB calculations, the inner shell orbitals of C, Si, and Cl are frozen at the Hartree−Fock level, while all the valence shell orbitals are optimized in both the VBSCF and BOVB methods. For the sake of simplicity and to be consistent with the optimization method for the reaction coordinate, the VB curves are calculated in terms of energies rather than free energies, and the thermal corrections are applied only to the ground state minimum and the bond dissociation limit. Given that the so-calculated free energy trends follow the energy trends, our underlying expectation in the present paper is that the same energy/free energy correlation carries over to the comparison of the curve crossing and avoided crossing.

Results

The Dissociation of $(CH_3)_3C-Cl$. The dissociation energies of $(CH_3)_3C-Cl$ in gas and in water phase, as computed by ab initio VB and MO methods, are shown in Table 1. Columns 1 and 3 refer to reaction enthalpies, while free energies with thermal corrections at ambient temperature are reported in columns 2 and 4. It is seen that the free energies are lower than the energies by a considerable amount due to the increase of degrees of freedom upon dissociation.

Because the CCSD(T) level of theory is known to provide dissociation energies that are close to the complete electron correlation limit within a given basis set, this level will be taken hereafter as the reference against which other computational levels will be compared. Indeed, it can be seen from Table 1 that the CCSD(T)/6-31G(d) value for the dissociation energy in gas-phase is close to the experimental value, the difference of 5 kcal/mol being quite normal owing to our medium-sized basis set. On the other hand, it can be seen that the Hartree−Fock value is too small, showing the importance of electron correlation, such that the accuracy of the VB results follows the hierarchy of the VB levels. The L- and D-VBSCF levels involve some nondynamic correlation but still lack the dynamic correlation that is essential for getting reliable bonding energies. Remarkably, the D-option, which describes properly the interactions between spectator orbitals (C−C bonds, C−H bonds, and chlorine lone pairs) by letting them freely delocalize, appears as necessary, as was found to be the case in previous studies of carbon−halogen bonds.[22a,b] The BOVB levels, which involve some dynamic correlation, are much improved with respect to VBSCF, and the D-BOVB value is close to the CCSD(T) one within 5 kcal/mol. A still better VB level, the so-called SD-BOVB, would probably yield a gas-phase dissociation energy even closer to CCSD(T); however, as it has been argued in the theoretical section, this extra complexity is not needed for the calculation of heterolytic dissociation energies, which are the only quantities of interest for the scope of the present work. Indeed, the VBPCM//D-BOVB results for the heterolytic dissociation in water phase (columns 3 and 4) are in excellent agreement with the CCSD(T)/PCM result and with experiment.[1]

Our results can be compared with the results of other studies, such as those using reaction field models[8,25,26] (Table 1, entries 7 and 8), in which the solvent is treated as a structureless dielectric continuum, as in the present work, and those considering solvent molecules explicitly (Table 1, entries 9−15). In the framework of continuum solvation models, Ford and Wang[25] generated a reaction profile that rises quasi-continuously up to an energy of 20.5 kcal/mol for the free ion pair except for a very shallow intermediate minimum. Very similar results were obtained by Kikuchi et al. at the ab initio (MP2) level within a continuum solvation model, yielding a dissociation energy of ∼20 kcal/mol and practically no minimum.[26] These two results, which are based on MO theory, are in excellent agreement with our VBPCM//D-BOVB dissociation energy (Table 1, entry 4) and with the shape of our dissociation curve for t-BuCl (see below).

Theoretical studies considering solvent molecules explicitly are of the semi-empirical type,[27−32] except for ab initio or DFT calculations[33,34] with a small number of H_2O molecules. Jorgensen et al.[27] determined the free energy profile of the ion pair region using free energy perturbation and Monte Carlo simulations. They concluded that the free energy barrier between the contact ion pair and the solvent separated ion pair is 2 kcal/mol and that the latter is lower in free energy that the contact ion pair. Merz et al[28] used the QM/MM method using the PM3 Hamiltonian for the tertiary-butyl chloride solute, which was surrounded by a large number of explicit water molecules. With a first computational scheme (Born correction), they obtained a deep minimum at the equilibrium bond length and a barrier of 17.8 kcal/mol for dissociation to $t\text{-}Bu^+Cl^-$. The contact ion pair was found to be stabilized in a well of depth 8.7 kcal/mol relative to separated ions, and a shallow minimum corresponding to the solvent separated ion pair was observed at 6.4 Å. With a second computational scheme (charge correction), the barrier to initial fragmentation was 23.4 kcal/mol, and the contact ion pair was only 0.5 kcal/mol below the TS.

Calculations of a similar type with further corrections of the solute energies at the ab initio level was performed by Watanabe et al.[29] Monte Carlo and statistical perturbation theories were

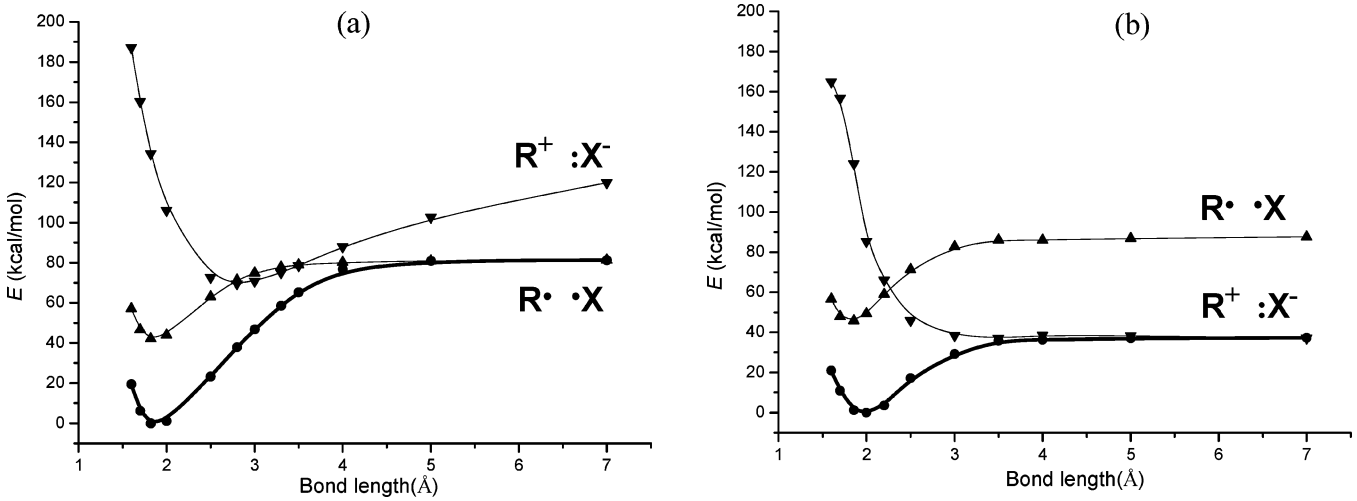

Figure 2. The dissociation curves of $(CH_3)_3CCl$ in gas phase (a) and in solvated phase (b).

carried out to calculate the free energy profile for the solvolysis reaction, yielding a barrier of 28.5 kcal/mol and a CIP lying ~25 kcal/mol above minimum t-BuCl.

Keirstead et al.[30] used an empirical two-state VB treatment to perform molecular dynamics simulation of the solvolysis reaction in liquid water. They found a barrier to CIP formation of 20 kcal/mol. Using a similar model but with more explicit water molecules, Rossky et al.[31] found a barrier to solvolysis of 23 kcal/mol and a CIP lying 7 kcal/mol below the TS. Still using an empirical VB approach, Winter et al.[32] performed a molecular dynamic study with 1000 water molecules, yielding a barrier of 20.5 kcal/mol and a CIP lying 4 kcal/mol below the TS.

As can be seen, all these dynamical or statistical semiempirical studies with one exception[29] yield consistent barriers to solvolysis in the range 20−23 kcal/mol but differ considerably on the stability of the CIP relative to the TS.

It is clear that because it does not yield an accurate description of the CIP and SSIP intermediates, the continuum solvation model is cruder than the Monte Carlo or molecular dynamic simulations. However, even these latter sophisticated methods disagree with each other on the stability of the CIP. On the other hand, the continuum solvation models provide rather accurate values for the global energy that is requested to dissociate the C−Cl bond in water. Given that we are interested in the dissociation energy of the C−Cl and Si−Cl bonds in water rather than in the detailed interactions of the ions with the solvent molecule, the use of a continuum model appears as fully justified for the problem at hand.

Figure 2 shows the dissociation curves of $(CH_3)_3CCl$ in gas phase and in solvated phase, as calculated respectively at the D-BOVB and VBPCM//D-BOVB levels with the basis set mentioned above. The corresponding D-VBSCF curves are relegated to Supporting Information. The figures include the ground state (adiabatic profile) and the individual covalent and ionic structures (diabatic profiles). In the gas phase (Figure 2a), the covalent curve is below the ionic at the equilibrium bond distance, indicating a dominant covalent character for the C−Cl bond. The covalent curve displays a potential well of ca. 39 kcal/mol and reaches a plateau beyond a distance of 3−4 Å. The ionic curve is also attractive, but its minimum is shifted to a longer C−Cl distance (ca. 2.8 Å) relative to the covalent one, so that the two curves become quasi-degenerate in the range 2.8−3.4 Å. At longer distances, the lowest energy curve is the covalent curve, thus leading to two radical products (actually, a lower energy pathway in the gas phase leads to an elimination reaction and production of HCl and iso-butene). It is noteworthy that the covalent-ionic resonance energy (RE_{C-I}), which is the energy gap between the ground state and the lowest of the two diabatic curves, diminishes with the increase of the interatomic distance, as predicted by theory because the integral that couples the two diabatic states is exponentially dependent on the distance.[22a] At equilibrium distance, the RE_{C-I} quantity amounts to 42 kcal/mol at the D-BOVB levels, that is, about one-half of the total bonding energy (not thermally corrected) thus making the C−Cl bond in t-BuCl a borderline case inbetween charge-shift bonds and classical polar covalent bonds, as was found previously for the H_3C-Cl bond.[22a,b]

Comparison of Figures 2a,b shows that the covalent dissociation curve is hardly changed from gas phase to aqueous phase, as expected becasue the purely covalent component of the C−Cl bond is nonpolar by definition. On the other hand, solvation has a major effect on the ionic curve, which is globally lowered and becomes repulsive. The ionic curve crosses the covalent one at a C−Cl distance of ca. 2.3 Å and becomes the ground state at long distance, leading smoothly to separate ions. As a consequence of the lowering of the ionic structure, the equilibrium C−Cl bond length in water is stretched by ca. 0.2 Å compared to the gas-phase value. Another expected consequence of the ionic structure lowering in aqueous phase is a decrease of the covalent-ionic gap at short interatomic distances, leading to a substantial covalent-ionic resonance energy, 49 kcal/mol, at the equilibrium distance compared with 42 kcal/mol in the gas phase. Even if only part of RE_{C-I} enters the barrier, it is apparent from the curves displayed in Figure 2b that the root cause for the activation energy required in the S_N1 process is precisely this large covalent-ionic resonance energy at equilibrium distance and its diminishment as the fragments separate from each other. Thus, the origin of the S_N1 barrier is not the height of the crossing point, but rather it is the loss of the covalent-ionic resonance energy of the bond.

This physical picture provided by the diabatic dissociation curves is further illustrated by the evolution of the calculated weights for the covalent and ionic structures as a function of the reaction coordinate, Figure 3. In the gas phase (Figure 3a), it can be seen that the covalent structure is the major one at short and long distances but has about the same weight as the ionic one for a C−Cl distance range of ca. 2.8−3.5 Å, corresponding to the diabatic surface crossing in Figure 2a. In water phase (Figure 3b), the nature of the C−Cl bond is

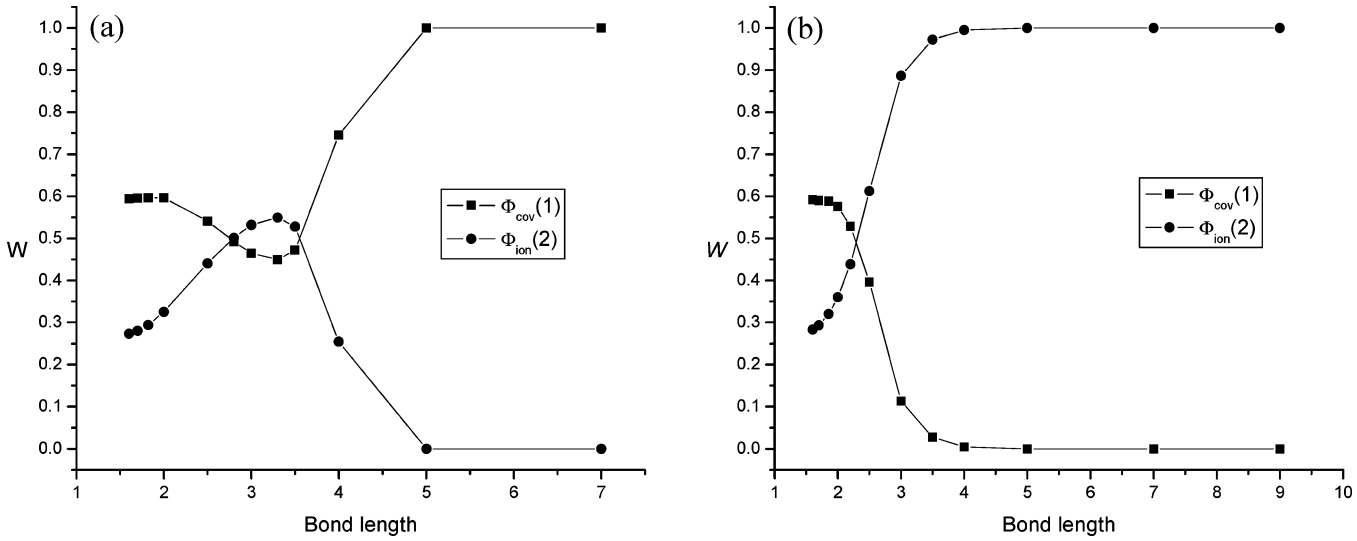

Figure 3. Weights of VB structures for $(CH_3)_3C-Cl$ in gas phase (a) and in solvated phase (b) as a function of the dissociation coordinate, as calculated by the D-BOVB method. Bond lengths in Å.

TABLE 2: The Dissociation Energy[a] and Dissociation Free Energy[a] of $(CH_3)_3Si-Cl$, in Gas Phase and Aqueous Phase

	gas phase		aqueous phase	
	D_e (kcal/mol)	G^b (kcal/mol)	D_e (kcal/mol)	$G^{c,d}$ (kcal/mol)
D-VBSCF	96.6	85.9	52.9	41.1
D-BOVB	103.1	92.4	62.0	50.2
HF	92.9	82.2	41.3	29.5
MP2	111.9	101.2	52.7	40.9
CCSD(T)	108.2	97.5	52.6	40.8

[a] Energies in kcal/mol. [b] Thermal correction in VB and MO results come from MP2/6-31G(d). [c] Thermal correction in VB and MO results come from HF/IEFPCM/6-31G(d). [d] Nonelectrostatic solvation free energy terms come from HF/IEFPCM.

practically the same as in gas phase at equilibrium distance, a polar bond with a covalent/ionic ratio of about 65/25 (note that the minor ionic structure, $(CH_3)_3C^-\ Cl^+$, is not represented). On the other hand, the situation changes drastically at larger distances, and the ionic structure becomes predominant from a C−Cl distance of 2.2 Å onward.

The Dissociation Process for $(CH_3)_3SiCl$. Table 2 displays the calculated dissociation energies for $(CH_3)_3SiCl$ with and without thermal corrections. There are no experimental values for the dissociation leading to free ions in water, because faster reactions with the solvent take place under experimental conditions, which is precisely the reason why free silylium ions in solution are very difficult to probe.[10] Because the D-computational option has proved definitely necessary for the problem at hand (vide supra), only the results of the D-VBSCF and D-BOVB levels are reported for the VB calculations for $(CH_3)_3SiCl$.

As was found in the t-BuCl case (Table 1), the accuracy of the various computational levels increases in the order Hartree−Fock, D-VBSCF, D-BOVB, MP2, relative to the CCSD(T) level taken as a reference, and the D-BOVB level provides a heterolytic dissociation energy close to the CCSD(T) one in water phase.

The thermally corrected homolytic dissociation energy of $(CH_3)_3SiCl$ is calculated to be 97.5 kcal/mol at the CCSD(T) level (Table 2) versus 67.3 kcal/mol for t-BuCl (Table 1), which is in harmony with the well-known fact that the Si−Cl bond is stronger than the C−Cl one.[5a−c,22a,b] Similarly, the theoretical value for the heterolytic dissociation in water is calculated to be much larger for $(CH_3)_3SiCl$ than for t-BuCl. Indeed, had it not been for alternative reactions of $(CH_3)_3SiCl$ in water (e.g., nucleophilic attack by the solvent and formation of pentacoordinated intermediates en route to hydrolysis), the heterolytic dissociation by itself would have required to surmount a barrier of 40.8 kcal/mol (Table 2, CCSD(T) level, entry 5), and thus be prohibitively slow. This raw computational result by itself accounts very well for the rarity of free silylium ions in water and more generally in polar solvents. Now we need to understand what physical reason makes the Si−Cl heterolytic dissociation so difficult in solution. This insight is provided by the diabatic and adiabatic dissociation curves displayed in Figures 4 (the analogous VBSCF curves are given in Supporting Information).

The most striking feature of the gas-phase dissociation curves for $(CH_3)_3SiCl$, displayed in Figure 4a, is the position of the ionic curve relative to the covalent one. Although the ionic curve was generally higher than the covalent one in the t-BuCl case (see Figure 2a), here the two diabatic curves are nearly degenerate at equilibrium distance, and the ionic structure becomes the lowest one in a larger region of the reaction coordinate from 2.1 to 5.3 Å. Subsequently, the ionic curve crosses the covalent one a second time and goes up while the covalent curve reaches a plateau and leads to the separate free radicals. Another feature of the ionic curve in Figure 4a is the very tight minimum $(CH_3)_3Si^+\ Cl^-$ at 2.3 Å compared with 2.8 Å for the corresponding $(CH_3)_3C^+\ Cl^-$ (Figure 2a). Thus, as we already noted,[22a,b] the silicenium cation $(CH_3)_3Si^+$ is considerably smaller than the tertiarybutyl cation $(CH_3)_3C^+$ by as much as 0.5 Å! This is also the root cause of the deeper $(CH_3)_3Si^+\ Cl^-$ minimum (Figure 4a) compared with $(CH_3)_3C^+\ Cl^-$ (Figure 2a). These features of the ionic structure are fundamental and will be elaborated further in the discussion section.

Finally, a noticeable difference between the gas-phase curves in Figure 4a versus 2a is the covalent-ionic resonance energy that is larger in $(CH_3)_3SiCl$ than in t-BuCl (61 versus 42 kcal/mol at the D-BOVB level). The cause of this difference is the above-mentioned tightness of the $(CH_3)_3Si^+Cl^-$ minimum, which is shorter by ca. 0.5 Å than the $(CH_3)_3C^+Cl^-$ minimum. Because the covalent-ionic resonance energy is proportional to the overlap of the orbitals on $(CH_3)_3E$ and Cl (E = C, Si),[37] the shorter distance between R_3Si^+ and the counterion is consistent

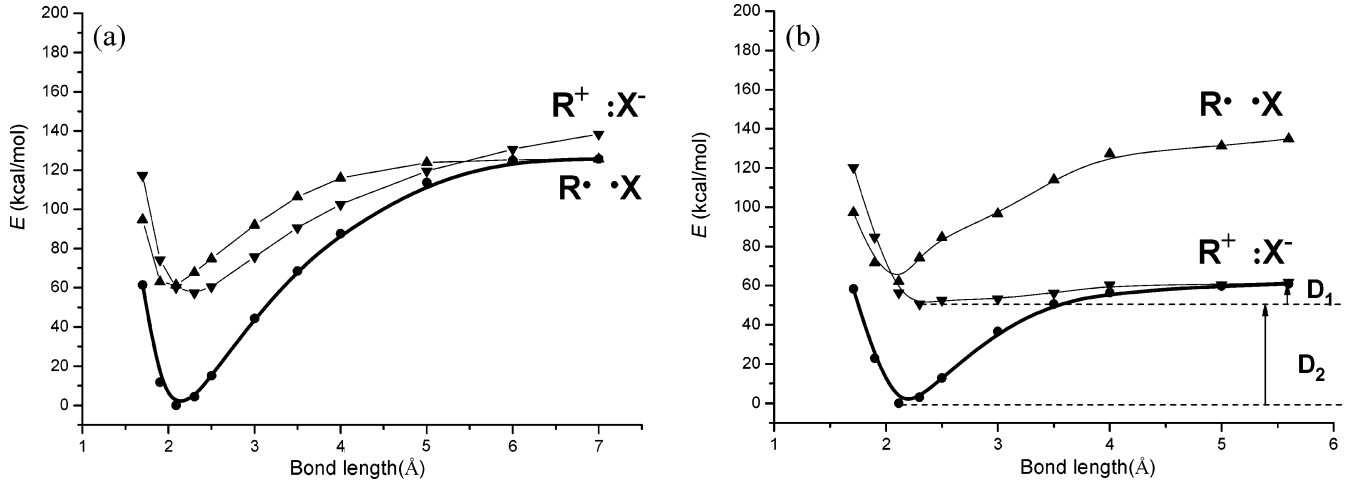

Figure 4. The dissociation curves of $(CH_3)_3SiCl$ in gas phase (a) and in solvated phase (b).

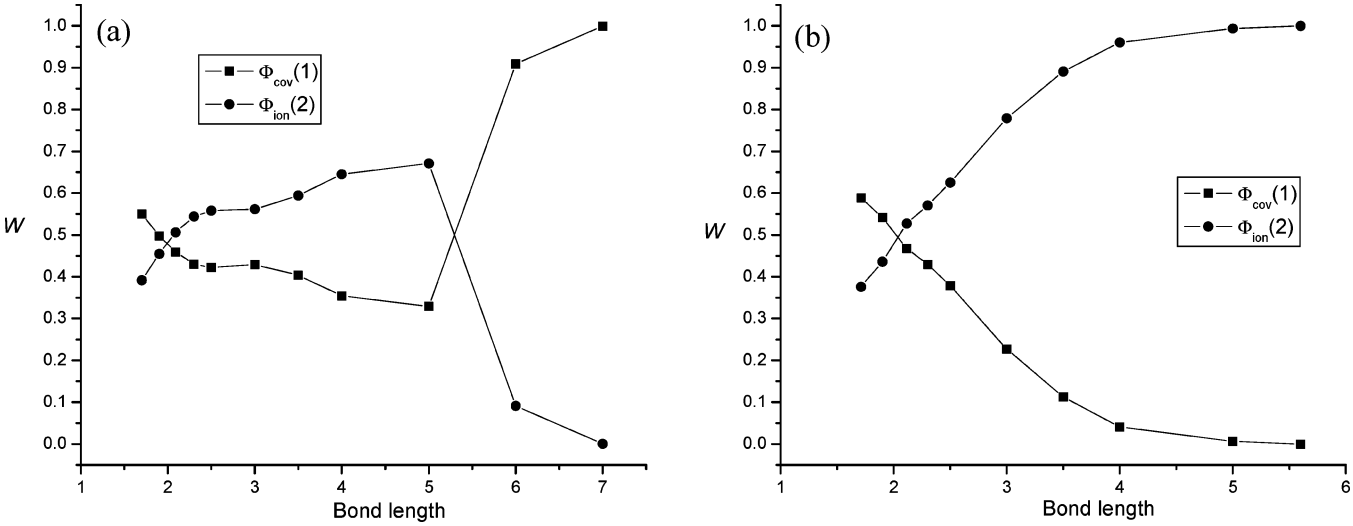

Figure 5. Weights of VB structures for $(CH_3)_3Si-Cl$ in gas phase (a) and in aqueous phase (b) as a function of the dissociation coordinate, as calculated by the D-BOVB/PCM method. Bond lengths in Å.

with the larger value of the covalent-ionic resonance energy in $(CH_3)_3SiCl$. Therefore, the Si−Cl bond is confirmed to have a significant charge-shift character, as was found in an earlier study of the H_3SiCl case in which the electronic coupling between the covalent and ionic curves in the vicinity of the equilibrium geometry is effectively shown to be larger for the Si−Cl bond compared with C−Cl.[22a] How does this large resonance energy impact the behavior in aqueous solution?

The dissociation curves for $(CH_3)_3SiCl$ in water phase are displayed in Figure 4b. The minimum of the covalent curve is practically not affected by solvation and is located at the same Si−Cl distance and has almost the same absolute energy as in the gas phase (Figure 4a). On the other hand, the ionic curve is affected in two ways: (i) as for the carbon analog, the shape of the ionic curve for Si−Cl is flattened at large distances. However, by contrast to the $t\text{-}Bu^+Cl^-$ curve that is repulsive at all distances (see Figure 2b), the $(CH_3)_3Si^+Cl^-$ curve still displays a significant minimum. (ii) The $(CH_3)_3Si^+Cl^-$ minimum is stabilized by the solvent by 12.6 kcal/mol relative to the gas-phase ionic minimum and is slightly shifted to a longer distance. A consequence of this energy lowering is that the ionic curve becomes the lowest for much of the internuclear distance, and at its minimum the energy gap to the covalent structure is increased somewhat relative to the gas phase. This increase of the gap causes a modest decrease in the RE_{C-I} quantity, which now amounts to 57 versus 62 kcal/mol in the gas phase. Note that near the covalent minimum the RE_{C-I} quantity is larger (ca. 70 kcal/mol). Thus, our hypothesis expressed in a previous work[22] that the charge-shift character of the Si−Cl bond survives in solution appears to be confirmed.

The evolution of the covalent and ionic weights along the reaction coordinate, shown in Figure 5, is in agreement with the relative positions of the diabatic curves in both gas phase and aqueous phase. In the gas phase, the $(CH_3)_3Si-Cl$ bond is predominantly covalent at short distances; then the ionic/covalent ratio increases to a value of 50:50 at a distance corresponding to the equilibrium geometry. At larger distances, the ionic structure is predominant up to a distance of ca. 5.4 Å, which closely corresponds to the crossing of the diabatic structures in Figure 4a, then vanishes as the Si−Cl bond is further stretched, as expected for a homolytic dissociation. In aqueous solution (Figure 5b), the picture is simpler: the ionic structure has the lowest weight at distances shorter than 2 Å, but it subsequently dominates the wave function throughout the bond distances beyond 2 Å, while the covalent weight gradually collapses to zero at large distances.

Discussion

The main points we set to understand are the reasons why Si−X bonds do not undergo heterolysis in solution and why it is so difficult to generate a free silicenium ion in the condensed

TABLE 3: The Solvation Energies of the Free Ions and of the Ion Pairs in the Geometries of Their Gas-Phase Minima

	ΔG_{sol} (kcal/mol)
	HF
$(CH_3)_3Si^+$	−53.3
$(CH_3)_3C^+$	−55.0
Cl^-	−77.3
$(CH_3)_3Si^+Cl^-$	−12.6
$(CH_3)_3C^+Cl^-$	−32.3

phases? Part of the answer is already given in Figures 2 and 4, but not everything is given. Thus, to aid the discussion we provide in Table 3 the solvation energies of the free ions and of the ion pairs (in their gas-phase minima).

The classical explanation that is employed to account for the fact that uncoordinated R_3Si^+ cations are not detected in solution as opposed to the common R_3C^+ cations is two-fold.[8,10b,11] Thus, it is argued[10b] that Si−X bonds (X = electronegative leaving group) are stronger than equivalent C−X bonds. In addition, it is postulated that silicenium ions are solvated to a lesser extent than their carbenium analogs, because the positive charge is localized on the Si atom in R_3Si^+ and delocalized on the substituents in R_3C^+. Our data support the relative bond strengths; R_3Si−Cl bond is stronger than the R_3C−Cl bond, and in the present case the dissociation energies are respectively 97.5 versus 67.3 kcal/mol, as calculated at the CCSD(T) level in the gas phase. However, the strength of the bond, as estimated from the homolytic dissociation energy in the gas phase, is of little consequence if the ionic curve is more stabilized and becomes the ground state already at short distances (Figures 2b and 4b). Regarding the solvation argument, our data in Table 3 do not support the postulate that silicenium cations are much less solvated than carbenium ions. The data shows that at least in the case of the $(CH_3)_3C^+$ and $(CH_3)_3Si^+$ there is hardly any difference in the solvation energies. The fundamental difference between the two systems must lie elsewhere.

Comparison of Figures 2b and 4b shows that the carbon and silicon cases are quite different in this respect. Thus, the ionic curve $R_3C^+Cl^-$ is repulsive and leads smoothly to the free ions (Figure 2b), whereas the $R_3Si^+Cl^-$ curve displays a minimum, which is 12.6 kcal/mol deeper than the ionic dissociation limit (D_1 in Figure 4b). The data in Table 3 show that the retention of a relatively deep ion-pair minimum energy in the $R_3Si^+Cl^-$ curve is because the original gas-phase minimum is rather deep (143.3 kcal/mol), such that the increasing solvation energy that peaks at the asymptote of the free ions is insufficient to suppress this minimum. By contrast, in the $R_3C^+Cl^-$ case the original gas-phase minimum is more shallow (94.8 kcal/mol) and the solvation energy that increases as the distance between the ions increases is sufficient to abate this minimum. However, the shallow ionic potential well is not a dominant factor in the heterolysis, because this factor is much smaller than the dissociation barrier in Figure 4b. Indeed, it can be seen in Figure 4b that the ionic minimum is significantly lower in energy than the covalent one in solution. Therefore, if the covalent-ionic resonance energy would have been small the heterolytic energy barrier to generate the solvated free R_3Si^+ and Cl^- ions would have been moderate and the process as a whole would have become a feasible process at ambient temperature. However, the covalent-ionic resonance energy, RE_{C-I}, for Si−Cl at equilibrium geometry is very large, being 57 kcal/mol relative to the ionic structure. As may be seen from Figure 4b, the RE_{C-I} at the geometry of the ionic minimum still amounts to 50.7 kcal/mol (D_2 in Figure 4b), a quantity that fully enters the activation barrier for bond heterolysis, because this resonance energy

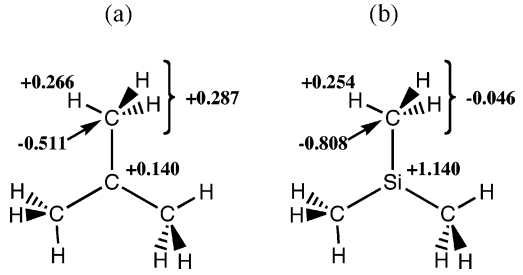

Figure 6. Mulliken net charges for the t-butyl (a) and trimethylsylil (b) cations in the gas phase, as calculated at the HF level in 6-31G(d) basis set.

stabilization is lost as the fragments are pulled apart to infinity. Thus, in terms of energies the contributions (uncorrected for thermal effects) to the total heterolytic dissociation energy in water are 12.6 kcal/mol (20%) due to residual electrostatic stabilization, and a large quantity of 50.7 kcal/mol (80%) due to the loss of the covalent-ionic resonance energy.

The above discussion shows that in both the carbon and silicon cases, the barrier for $(CH_3)_3E$-Cl heterolysis is due to the loss of the covalent-ionic resonance energy. However, in the $(CH_3)_3C$−Cl case, this quantity displays its maximum at the equilibrium geometry, relative to the covalent minimum that is higher than the ionic asymptote. Consequently, the ground-state minimum is not much lower in energy than the ionic asymptote, and the dissociation is a facile process that can occur at room temperature. On the other hand, in the $(CH_3)_3Si$−Cl case the covalent-ionic resonance energy is not only larger than in the preceding case, but this quantity is now fully expressed in the barrier because it refers to the ionic curve, which is the lowest one from the equilibrium geometry all the way to dissociation. Unlike the C−Cl heterolysis where only part of the RE_{C-I} enters the heterolytic dissociation barrier in Si−Cl, all the resonance energy contributes to the dissociation energy.

The root cause for the larger RE_{C-I} of the Si−Cl bond relative to the C−Cl one can be can be linked to the properties of the R_3Si^+ ion relative to R_3C^+. As argued before,[10b,22b,37b] the tighter ionic minimum of the $R_3Si^+Cl^-$ ion pair and its deeper stabilization energy compared with $R_3C^+Cl^-$ are rooted in the distribution of net charges in the two cations. Indeed, as shown in Figure 6, the net charges are clearly delocalized in R_3C^+ (+0.140 for carbon and +0.287 for each methyl group) while they are by contrast strictly localized in R_3Si^+ (+1.140 for silicon and −0.046 for each methyl group). Because the positive charge accumulates on Si along the bond axis, the counterion can approach R_3Si^+ at a shorter distance than in the carbon analog thus leading to a tighter minimum for $R_3Si^+Cl^-$ and a stronger electrostatic interaction compared with the $R_3C^+Cl^-$ analog (see Figures 4a versus 2a above). Furthermore, because the RE_{C-I} is very sensitive to the E-Cl distance,[37] this Si−Cl bond maintains in solution a larger RE_{C-I} than the C−Cl bond. The heterolysis barriers follow the order in the respective RE_{C-I} quantities of the two bonds.

Conclusion

The VBPCM calculations reveal the different natures of the C−Cl and Si−Cl bonds and account for the fact that t-BuCl undergoes facile heterolysis in solution, whereas the analogous $(CH_3)_3SiCl$ compound would not undergo heterolysis in aqueous solution (and will prefer the associative mechanism for the hydrolysis). The calculations show that the barriers for the heterolysis processes in both cases are controlled by the resonance energy (RE_{C-I}) between the ionic and covalent

components of the respective E−Cl bonds (E = C, Si) near their minima. Thus, the barrier is due to the loss of the RE_{C-I} as the bond undergoes dissociation. In the case of Si−Cl, the ionic structure is highly stable and crosses very early below the covalent curve and therefore, 100% of the RE_{C-I} contributes to the heterolysis barrier. By comparison, in the C−Cl case the ionic structure is intrinsically less stabilized, and it crosses later the covalent curve such that only part of the RE_{C-I} enters the activation barrier. Because the Si−Cl bond initially possesses a larger RE_{C-I} than the C−Cl bond, this and the enhanced stability of the ionic structure of Si−Cl near the equilibrium distance of the bond in solution cause a much larger heterolytic barrier for Si−Cl.

The postulated lesser solvation of the silicenium ion is not supported at least for the trimethylsilicenium case studied here; the two ions are solvated to the same extent (Table 3). It follows that the difference in the heterolysis barriers constitutes a measure of the relative RE_{C-I} quantities of the respective bonds, and the larger barrier for Si−Cl heterolysis is a plain manifestation of the charge-shift character of the Si−Cl bond.

The fact that R_3Si^+ ions are rare in condensed phases is associated precisely with the same factors. Thus, the charge in R_3Si^+ is localized on the Si atom (Figure 6), and in R_3C^+ the charge is completely delocalized. This makes the silicenium ion much smaller than the corresponding carbenium ion (by ca. 0.5 Å), and as such the ionic distance in $R_3Si^+X^-$ would always be shorter than the corresponding one in the carbon analog. The short distance to the counterion causes large covalent-ionic resonance energy in the Si−X cases and significantly less so in the C−X cases. Thus, the charge-shift character of the Si−X bond is expected to be general, and in a condensed phase any counterion or a polar molecule will tend to "stick" to the R_3Si^+ cation making it very difficult to generate free silicenium ions.[10,11]

As shown in a recent study,[49] the loss of the covalent-ionic resonance energy is the root cause of the experimental findings that halogen transfer reactions $H + XH' \rightarrow HX + H'$ have much larger barriers (by >20 kcalmol for X = F) than the corresponding hydrogen transfer processes $X + HX' \rightarrow XH + X'$, despite the similarity of the bonds that are broken or made in both reactions. It appears from the present study that the reluctance of R_3Si-X bonds to undergo heterolysis in solution and by way of consequence the rarity of the ionic chemistry of Si−X compounds is another experimental manifestation of charge-shift bonding. It is probable that further manifestations of this bonding mechanism in structure and reactivity are yet to be discovered.

Charge-shift bonds with large covalent-ionic resonance energy are quite ubiquitous and exist in a variety of molecules.[48] There are charge-shift homopolar bonds of electronegative and lone-pair rich atoms (e.g., F−F, Cl−Cl, O−O, S−S, etc.), as well as charge-shift heteropolar bonds involving electronegative and lone-pair rich elements bonded, for example, to second and third row metalloids (Si, Ge, Sn, etc.). Similarly, many of the heteropolar bonds of first-row transition metals, hypercoordinated species, such as PCl_5, SF_n ($n = 4, 6$), and so on;[48] all of these are charge-shift bonds. As this and the recent study[49] show, it is possible to identify experimental probes of this bonding feature and to chart this bonding territory.

Acknowledgment. The research at XMU is supported by the Natural Science Foundation of China (No. 20533020) and The National Basic Research Program of China (2004CB719902). The research at HU is supported in part by an Israel Science Foundation (ISF) grant to SS.

Supporting Information Available: Theory and methodology, VB procedures, VBPCM solvation model, and computational details are described in detail along with radii values of CH_3, Cl, C, and Si in $(CH_3)ECl$ (E = C, Si), dissociation curves, and full references for Gaussian and Gamess packages. This material is available free of charge via the Internet at http://pubs.acs.org.

References and Notes

(1) (a) Winstein, S.; Clippinger, E.; Fainberg, A. H.; Robinson, G. C.; *J. Amer. Chem. Soc.* **1954**, *76*, 2597. (b) Winstein, S.; Fainberg, A. H. *J. Amer. Chem. Soc.* **1957**, *79*, 5937.

(2) Abraham, M. H. *Prog. Phys. Org. Chem.* **1974**, *11*, 1.

(3) Abraham, M. H. *J. Chem. Soc., Perkin Trans. 2* **1973**, 1893.

(4) Kessler, H.; Feigel, M. *Acc. Chem. Res.* **1982**, *15*, 2.

(5) (a) Apeloig, Y. In *The Chemistry of Organic Silicon Compounds*; Patai, S., Rappoport, Z., Eds.; Wiley and Sons: Chischester, U.K., 1989; Chapter 2, pp 57. (b) Apeloig, Y. *Stud. Org. Chem.* **1987**, *31*, 33. (c) Apeloig, Y.; Merin-Aharoni, O. *Croat. Chem. Acta* **1992**, *65*, 757. (d) For a discussion of gas phase properties of silicenium ions, see: Schwarz, H. In *The Chemistry of Organic Silicon Compounds*; Patai, S., Rappoport, Z., Ed.; Wiley and Sons: Chischester, U.K., 1989; Vol 1, Chapter 7.

(6) Corriu, R. J. P.; Henner, M. *J. Organomet. Chem.* **1974**, *74*, 1.

(7) Eaborn, C. In *Organosilicon and Bioorganosilicon Chemistry*; Sakurai, H., Ed.; Ellis Horwood: U.K., 1985.

(8) Olah, G. A.; Heiliger, L.; Li, X. -Y.; Prakash, G. K. S. *J. Amer. Chem. Soc.* **1990**, *112*, 5991.

(9) Lickiss, P. D. *J. Chem. Soc., Dalton Trans.* **1992**, 1333.

(10) For a few reviews on the elusive R_3Si^+ cation in condensed phases, see: (a) Y. Apeloig, A. Stanger, *J. Am. Chem. Soc.* **1987**, *109*, 272. (b) Y. Apeloig, *Stud. Org. Chem.* **1987**, *31*, 33. (c) J. B. Lambert, L. Kania, S. Zhang, *Chem. Rev.* **1995**, *95*, 1191. (d) Gaspar, P. P. *Science* **2002**, *297*, 785.

(11) Prakash, G. K. S.; Keyaniyan, S.; Aniszfeld, R.; Heiliger, L.; Olah, G. A.; Stevens, R. C.; Choi, H. -K.; Bau, R. *J. Amer. Chem. Soc.* **1987**, *109*, 5123.

(12) (a) Gomes de Mesquita, A. H.; MacGillavry, C. H.; Eriks, K. *Acta Cryst.* **1965**, *18*, 437. (b) Olah, G. A. *Top. Curr. Chem.* **1979**, *80*, 19.

(13) (a) Lambert, J. B.; Zhao, Y. *Angew. Chem., Int. Ed.* **1997**, *36*, 400. (b) Kim, K.-C.; Reed, C. A.; Elliott, D. W.; Mueller, L. J.; Tham, F.; Lin, L.; Lambert, J. B. *Science* **2002**, *297*, 825. (c) Belzner, J. *Angew. Chem., Int. Ed.* **1997**, *109*, 1331. (d) Lambert, J. B.; Lin, L. J.; Keinan, S. *Org. Biomol. Chem.* **2003**, *1*, 2559.

(14) For a two-coordinate silyl cation stabilized by aromaticity, see: Driess, M.; Yao, S.; Brym, M.; van Wüllen, C. *Angew. Chem., Int. Ed.* **2006**, *45*, 6730.

(15) For silylium ions stabilized by conjugation with multiple bonds, see: (a) Ichinohe, M.; Igarashi, M.; Sanuki, K.; Sekiguchi, A. *J. Amer. Chem. Soc.* **2005**, *127*, 9978. (b) Sekiguchi, A.; Matsuno, T.; Ichinohe, M. *J. Amer. Chem. Soc.* **2000**, *122*, 11250.

(16) For silylium ions stabilized by Si−X−Si three-center bonds, see: Panisch, R.; Bolte, M. Müller, T. *J. Amer. Chem. Soc.* **2006**, *128*, 9676. (b) Khalimon, A. Y.; Lin, Z. H.; Simionescu, R.; Vyboishchikov, S. F.; Nikonov, G. I. *Angew. Chem., Int. Ed.* **2007**, *46*, 4530. (c) Sekiguchi, A.; Murakami, Y.; Fukaya, N.; Kabe, Y. *Chem. Lett.* **2004**, *33*, 530.

(17) (a) Ogg, R. A.; Polanyi, M. *Trans. Faraday Soc.* **1935**, *31*, 604. (b) Evans, A. G. *Trans. Faraday Soc.* **1946**, *42*, 719.

(18) Warshell, A.; Weiss, R. M. *J. Amer. Chem. Soc.* **1980**, *102*, 6218.

(19) Shaik, S.; Pross, A. *Acc. Chem. Res.* **1983**, *16*, 363.

(20) (a) Hynes, J. T.; Mathis, J. R. *J. Phys. Chem.* **1994**, *98*, 5445. (b) Kim, H. J.; Hynes, J. T. *J. Am. Chem. Soc.* **1992**, *114*, 10508. (c) Kim, H. J.; Hynes, J. T. *J. Amer. Chem. Soc.* **1992**, *114*, 10528. (d) Mathis, J. R.; Kim, H. J.; Hynes, J. T. *J. Amer. Chem. Soc.* **1993**, *115*, 8248.

(21) Peters, K .S. *Acc. Chem. Res.* **2007**, *40*, 1.

(22) (a) Lauvergnat, D.; Hiberty, P. C.; Danovich, D.; Shaik, S. *J. Phys. Chem.* **1996**, *100*, 5715. (b) Shurki, A.; Hiberty, P. C.; Shaik, S. *J. Amer. Chem. Soc.* **1999**, *121*, 822. (c) Shaik, S.; Maitre, P.; Sini, G.; Hiberty, P. C. *J. Am. Chem. Soc.* **1992**, *114*, 7861−7866.

(23) Song, L.; Wu, W.; Zhang, Q.; Shaik, S. *J. Phys. Chem. A* **2004**, *108*, 6017.

(24) Shaik, S. *J. Org. Chem.* **1987**, *52*, 1563.

(25) Ford, G. P.; Wang, B. *J. Amer. Chem. Soc.* **1992**, *114*, 10563.

(26) Takahashi, O; Sawahala, H.; Ogawa, Y; Kikuchi, O. *J. Mol. Struc. (Theochem)* **1997**, *393*, 141.

(27) Jorgensen, W. L.; Buchner, J. K.; Huston, S. E.; Rossky, P. J. *J. Am. Chem. Soc.* **1987**, *109*, 1891.

(28) Hartsough, D. S.; Merz, K. M., Jr. *J. Phys. Chem.* **1995**, *99*, 384.

(29) Watanabe, T.; Kikuchi, O. *J. Phys. Chem. A* **2000**, *104*, 7840−7846.

(30) Keirstead, W. P.; Wilson, K. R.; Hynes, J. T. *J. Chem. Phys.* **1991**, *95*, 5256.
(31) Westacott, R. E.; Johnston, K. P.; Rossky, P. J. *J. Phys. Chem. B* **2001**, *105*, 6611.
(32) Winter, N.; Benjamin, I. *J. Chem. Phys.* **2005**, *122*, 184717.
(33) Okuno, Y. *J. Phys. Chem. A* **1999**, *103*, 190−196.
(34) Yamabe, S.; Tsuchida, N. *J. Comput. Chem.* **2004**, *25*, 598.
(35) Arshadi, M.; Johnels, D.; Edlund, U.; Ottosson, C.-H.; Cremer, D. *J. Am. Chem. Soc.* **1996**, *118*, 5120.
(36) Maerker, C.; Schleyer, P. v. R. In *The Chemistry of Organic Silicon Compounds*; Rappoport, Z., Apeloig. Y., Eds.; Wiley: Chichester, U.K., 1998; Vol. 2, pp 513−556.
(37) (a) Shaik, S.; Hiberty, P. C. *Adv. Quant. Chem.* **1995**, *26*, 99. (b) Shaik, S.; Shurki, A. *Angew. Chem., Int. Ed.* **1999**, *38*, 586. (c) Shaik, S.; Hiberty, P. C. *A Chemist's Guide to Valence Bond Theory*; Wiley-Interscience: New York, 2007.
(38) Song, L.; Wu, W.; Shaik, S.; Hiberty, P. C. *Chem.—Eur. J.* **2006**, *12*, 7458.
(39) Shurki, A.; Crown H. A. *J. Phys. Chem. B* **2005**, *109*, 23638.
(40) (a) Mo, Y.; Gao, J. *J. Comput. Chem.* **2000**, *21*, 1458. (b) Mo, Y.; Gao, J. *J. Phys. Chem.* **2000**, *104*, 3012.
(41) (a) Verbeek, J.; van Lenthe, J. H. *J. Mol. Struct.* (*Theochem*) **1991**, *229*, 115. (b) van Lenthe, J. H. *Int. J. Quant. Chem.* **1991**, *40*, 201. (c) Balint-Kurti, G. G.; Benneyworth, P. R.; Davis, M. J.; Williams, I. H. *J. Phys. Chem.* **1992**, *96*, 4346.
(42) (a) Hiberty, P. C.; Flament, J. P.; Noizet, E. *Chem. Phys. Lett.* **1992**, *189*, 259. (b) Hiberty, P. C.; Humbel, S.; Byrman, C. P.; van Lenthe, J. H. *J. Chem. Phys.* **1994**, *101*, 5969. (c) Hiberty, P. C.; Shaik, S. *Theor. Chem. Acc.* **2002**, *108*, 255.
(43) Chirgwin, H. B.; Coulson, C. A. *Proc. R. Soc. London, Ser. A* **1950**, *2*, 196.
(44) (a) Cances, M. T.; Mennucci, V.; Tomasi, J. *J. Chem. Phys.* **1997**, *107*, 3032. (b) Cossi, M.; Barone, V.; Mennucci, B.; Tomasi, J. *Chem. Phys. Lett.* **1998**, *286*, 253.
(45) Frisch, M. J.; Trucks, G. W.; Schlegel, H. B.; Scuseria, G. E.; Robb, M. A.; Cheeseman, J. R.; Zakrzewski, V. G.; Montgomery, J. A., Jr.; Stratmann, R. E.; Burant, J. C.; Dapprich, S.; Millam, J. M.; Daniels, A. D.; Kudin, K. N.; Strain, M. C.; Farkas, O.; Tomasi, J.; Barone, V.; Cossi, M.; Cammi, R.; Mennucci, B.; Pomelli, C.; Adamo, C.; Clifford, S.; Ochterski, J.; Petersson, G. A.; Ayala, P. Y.; Cui, Q.; Morokuma, K.; Malick, D. K.; Rabuck, A. D.; Raghavachari, K.; Foresman, J. B.; Cioslowski, J.; Ortiz, J. V.; Stefanov, B. B.; Liu, G.; Liashenko, A.; Piskorz, P.; Komaromi, I.; Gomperts, R.; Martin, R. L.; Fox, D. J.; Keith, T.; Al-Laham, M. A.; Peng, C. Y.; Nanayakkara, A.; Gonzalez, C.; Challacombe, M.; Gill, P. M. W.; Johnson, B. G.; Chen, W.; Wong, M. W.; Andres, J. L.; Head-Gordon, M.; Replogle, E. S.; Pople, J. A. *Gaussian 98*, revision 10; Gaussian, Inc.: Pittsburgh, PA, 1998.
(46) Schmidt, M. W.; et al. GAMESS. *J. Comput. Chem.* **1993**, *14*, 1347−1363.
(47) (a) Song, L.; Wu, W.; Mo, Y.; Zhang, Q. *XMVB: An Ab Initio Nonorthogonal Valence Bond Program*; Xiamen University: Xiamen, 1999. (b) Song, L.; Mo, Y.; Zhang, Q.; Wu, W. *J. Comput. Chem.* **2005**, *26*, 514.
(48) Shaik, S.; Danovich, D.; Silvi, B.; Lauvergnat, D.; Hiberty, P. C. *Chem.—Eur. J.* **2005**, *11*, 6358.
(49) Hiberty, P. C.; Mégret, C.; Song, L.; Wu, W.; Shaik, S. *J. Am. Chem. Soc.* **2006**, *128*, 2836.